Chapter 6

Unsteady Magnetohydrodynamic Flow of Jeffrey Fluid through a Porous Oscillating Rectangular Duct

Amir Khan, Gul Zaman and Obaid Algahtani

Additional information is available at the end of the chapter

http://dx.doi.org/10.5772/intechopen.70891

Abstract

This chapter presents some new exact solutions corresponding to unsteady magnetohydrodynamic (MHD) flow of Jeffrey fluid in a long porous rectangular duct oscillating parallel to its length. The exact solutions are established by means of the double finite Fourier sine transform (DFFST) and discrete Laplace transform (LT). The series solution of velocity field, associated shear stress and volume flow rate in terms of Fox H-functions, satisfying all imposed initial and boundary conditions, have been obtained. Also, the obtained results are analyzed graphically through various pertinent parameter.

Keywords: porous medium, Jeffrey fluid, oscillating rectangular duct, Fox H-function, MSC (2010): 76A05, 76A10

1. Introduction

Considerable progress has been made in studying flows of non-Newtonian fluids throughout the last few decades. Due to their viscoelastic nature non-Newtonian fluids, such as oils, paints, ketchup, liquid polymers and asphalt exhibit some remarkable phenomena. Amplifying interest of many researchers has shown that these flows are imperative in industry, manufacturing of food and paper, polymer processing and technology. Dissimilar to the Newtonian fluid, the flows of non-Newtonian fluids cannot be explained by a single constitutive model. In general the rheological properties of fluids are specified by their so-called constitutive equations. Exact recent solutions for constitutive equations of viscoelastic fluids are given by Rajagopal and Bhatnagar [1], Tan and Masuoka [2, 3], Khadrawi et al. [4] and Chen et al. [5] etc. Among non-Newtonian fluids the Jeffrey model is considered to be one of the simplest type of model which best explain the rheological effects of viscoelastic fluids. The Jeffrey model is a relatively simple linear model using the time derivatives instead of convected derivatives. Nadeem et al. [6] obtained analytic solutions for stagnation flow of Jeffrey fluid over a shrinking sheet. Khan [7] investigated partial slip effects on the oscillatory flows of fractional Jeffrey fluid in a porous medium. Hayat et al. [8]

examined oscillatory rotating flows of a fractional Jeffrey fluid filling a porous medium. Khan et al. [9] discussed unsteady flows of Jeffrey fluid between two side walls over a plane wall.

Much attention has been given to the flows of rectangular duct because of its wide range applications in industries. Gardner and Gardner [10] discussed magnetohydrodynamic (MHD) duct flow of two-dimensional bi-cubic B-spline finite element. Fetecau and Fetecau [11] investigated the flows of Oldroyd-B fluid in a channel of rectangular cross-section. Nazar et al. [12] examined oscillating flow passing through rectangular duct for Maxwell fluid using integral transforms. Unsteady magnetohydrodynamic flow of Maxwell fluid passing through porous rectangular duct was studied by Sultan et al. [13]. Tsangaris and Vlachakis [14] discussed analytic solution of oscillating flow in a duct of Navier-Stokes equations.

In the last few decades the study of fluid motions through porous medium have received much attention due to its importance not only to the field of academic but also to the industry. Such motions have many applications in many industrial and biological processes such as food industry, irrigation problems, oil exploitation, motion of blood in the cardiovascular system, chemistry and bio-engineering, soap and cellulose solutions and in biophysical sciences where the human lungs are considered as a porous layer. Unsteady MHD flows of viscoelastic fluids passing through porous space are of considerable interest. In the last few years a lot of work has been done on MHD flow, see [15–19] and reference therein.

According to the authors information up to yet no study has been done on the MHD flow of Jeffrey fluid passing through a long porous rectangular duct oscillating parallel to its length. Hence, our main objective in this note is to make a contribution in this regard. The obtained solutions, expressed under series form in terms of Fox H-functions, are established by means of double finite Fourier sine transform (DFFST) and Laplace transform (LT). Finally, the obtained results are analyzed graphically through various pertinent parameter.

2. Governing equations

The equation of continuity and momentum of MHD flow passing through porous space is given by [7]

$$\nabla \cdot V = 0, \rho\left(\frac{d\mathbf{V}}{dt}\right) = div\mathbf{T} + \mathbf{J} \times \mathbf{B} + \mathbf{R}, \tag{1}$$

where velocity is represented by **V**, density by ρ, Cauchy stress tensor by **T**, magnetic body force by $\mathbf{J} \times \mathbf{B}$, current density by **J**, magnetic field by **B,** and Darcy's resistance in the porous medium by **R**.

For an incompressible and unsteady Jeffrey fluid the Cauchy stress tensor is defined as [9]

$$\mathbf{T} = -p\mathbf{I} + \mathbf{S}, \quad \mathbf{S} = \frac{\mu}{1+\lambda}\left[\mathbf{A} + \theta\left(\frac{\partial \mathbf{A}}{\partial \mathbf{t}} + (\mathbf{V}.\nabla)\mathbf{A}\right)\right], \tag{2}$$

http://dx.doi.org/10.5772/intechopen.70891

where $\mathbf{S}$ and $p\mathbf{I}$ represents the extra stress tensor and the indeterminate spherical stress, the dynamic viscosity is denoted by μ, $\mathbf{A}=\mathbf{L}+\mathbf{L}^T$ is the first Rivlin-Ericksen tensor, $\mathbf{L}$ is the velocity gradient, λ is relaxation time and θ is retardation time. The Lorentz force due to magnetic field is

$$\mathbf{J}\times\boldsymbol{B}=-\sigma\beta_o^2\mathbf{V}, \tag{3}$$

where σ represents electrical conductivity and β_o the strength of magnetic field. For the Jeffrey fluid the Darcy's resistance satisfies the following equation

$$\mathbf{R}=-\frac{\mu\phi}{\kappa(1+\lambda)}\left(1+\theta\frac{\partial}{\partial t}\right)\mathbf{V}, \tag{4}$$

where $\kappa(>0)$ and $\phi(0<\phi<1)$ are the permeability and the porosity of the porous medium.

In the following problem we consider a velocity field and extra stress of the form

$$\mathbf{V}=(0,0,w(x,y,t)),\mathbf{S}=\mathbf{S}(x,y,t) \tag{5}$$

where w is the velocity in the z-direction. The continuity equation for such flows is automatically satisfied. Also, at $t=0$, the fluid being at rest is given by

$$\mathbf{S}(x,y,0)=\mathbf{0}, \tag{6}$$

therefore from Eqs. (2), (5) and (6), it results that $S_{xx}=S_{yy}=S_{yz}=S_{zz}=0$ and the relevant equations

$$\tau_1=\frac{\mu}{(1+\lambda)}\left(1+\theta\frac{\partial}{\partial t}\right)\partial_x w(x,y,t),\quad \tau_2=\frac{\mu}{(1+\lambda)}\left(1+\theta\frac{\partial}{\partial t}\right)\partial_y w(x,y,t), \tag{7}$$

where $\tau_1=S_{xy}$ and $\tau_2=S_{xz}$ are the tangential stresses. In the absence of pressure gradient in the flow direction, the governing equation leads to

$$(1+\lambda)\partial_t w(x,y,t)=\nu\left(1+\theta\frac{\partial}{\partial t}\right)\left(\partial_x^2+\partial_y^2\right)w(x,y,t)-\nu K\left(1+\theta\frac{\partial}{\partial t}\right)w(x,y,t)-H(1+\lambda)w(x,y,t), \tag{8}$$

where $H=\frac{\sigma B_0^2}{\rho}$ is the magnetic parameter, $K=\frac{\phi}{\kappa}$ is the porosity parameter and $\nu=\mu/\rho$ is the kinematic viscosity.

3. Statement of the problem

We take an incompressible flow of Jeffrey fluid in a porous rectangular duct under an imposed transverse magnetic field whose sides are at $x=0$, $x=d$, $y=0$, and $y=h$. At time $t=0^+$ the duct begins to oscillate along z-axis. Its velocity is of the form of Eq. (5) and the governing equation is given by Eq. (8). The associated initial and boundary conditions are

$$w(x,y,0) = \partial_t w(x,y,0) = 0, \tag{9}$$

$$w(0,y,t) = w(x,0,t) = w(d,y,t) = w(x,h,t) = Ucos(wt), \tag{10}$$

or

$$w(0,y,t) = w(x,0,t) = w(d,y,t) = w(x,h,t) = Usin(wt), \tag{11}$$

$$t > 0, 0 < x < d \text{ and } 0 < y < h.$$

The solutions of problems (8)–(10) and (8), (9), (11) are denoted by $u(x,y,t)$ and $v(x,y,t)$ respectively. We define the complex velocity field

$$F(x,y,t) = u(x,y,t) + iv(x,y,t), \tag{12}$$

which is the solution of the problem

$$(1+\lambda)\partial_t F(x,y,t) = \nu\left(1+\theta\frac{\partial}{\partial t}\right)\left(\partial_x^2+\partial_y^2\right)F(x,y,t) - \nu K\left(1+\theta\frac{\partial}{\partial t}\right)F(x,y,t) - H(1+\lambda)F(x,y,t), \tag{13}$$

$$F(x,y,0) = \partial_t F(x,y,0) = 0, \tag{14}$$

$$F(0,y,t) = F(d,y,t) = F(x,0,t) = F(x,h,t) = Ue^{iwt}, \tag{15}$$

$$t > 0, 0 < x < d \text{ and } 0 < y < h.$$

The solution of the problem (13)–(15) will be obtained by means of the DFFST and LT.

The DFFST of function $F(x,y,t)$ is denoted by

$$F_{mn}(t) = \int_0^d \int_0^h sin\left(\frac{m\pi x}{d}\right) sin\left(\frac{n\pi y}{h}\right) F(x,y,t)dxdy, \quad m,n = 1,2,3,.. \tag{16}$$

4. Calculation of the velocity field

Multiplying both sides of Eq. (13) by $sin\left(\frac{m\pi x}{d}\right)$ and $sin\left(\frac{n\pi y}{h}\right)$, integrating w.r.t x and y over $[0, d] \times [0, h]$ and using Eq. (16), we get

$$(1+\lambda)\frac{\partial F_{mn}(t)}{\partial t} + \nu\lambda_{mn}\left(1+\theta\frac{\partial}{\partial t}\right)F_{mn}(t) + H(1+\lambda)F_{mn}(t) + \nu K\left(1+\theta\frac{\partial}{\partial t}\right)F_{mn}(t)$$

$$= \nu\lambda_{mn}U\frac{[1-(-1)^m][1-(-1)^n]}{\zeta_m\lambda_n}(1+iw\theta)e^{iwt}, \tag{17}$$

where

http://dx.doi.org/10.5772/intechopen.70891

$$\zeta_m = \frac{m\pi}{d}, \lambda_n = \frac{n\pi}{h} \text{ and } \lambda_{mn} = \zeta_m^2 + \lambda_n^2.$$

The Fourier transform $F_{mn}(t)$ have to satisfy the initial conditions

$$F_{mn}(0) = \partial_t F_{mn}(0) = 0. \tag{18}$$

We apply LT to Eq. (17) and using initial conditions (18) to get

$$\overline{F}_{mn}(s) = \frac{\nu\lambda_{mn}U[1-(-1)^m](1+iw\theta)[1-(-1)^n]}{\zeta_m\lambda_n(s-iw)[(1+\lambda)(s+H)+\nu(1+\theta s)(\lambda_{mn}+K)]}. \tag{19}$$

We will apply the discrete inverse LT technique [20] to obtain analytic solution for the velocity fields and to avoid difficult calculations of residues and contour integrals, but first we express Eq. (19) in series form as

$$\begin{aligned}\overline{F}_{mn}(s) &= \frac{\nu\lambda_{mn}U[1-(-1)^m](1+iw\theta)[1-(-1)^n]}{\zeta_m\lambda_n(s-iw)}\sum_{p=0}^{\infty}\sum_{q=0}^{\infty}\sum_{r=0}^{\infty}\sum_{s=0}^{\infty}\sum_{l=0}^{\infty}\\ &\times\frac{\nu^{p+1}\lambda^s\theta^q K^{p-r}H^l(\lambda_{mn})^{r+1}\Gamma(q-p)\Gamma(r-p)\Gamma(s+p+1)\Gamma(l+p+1)}{(-1)^{-(p+q+r+s+l)}q!r!s!l!\Gamma(p)\Gamma(p)\Gamma(1+p)\Gamma(1+p)s^{l-q+p+1}}.\end{aligned} \tag{20}$$

We apply the discrete inverse LT to Eq. (20), to obtain

$$\begin{aligned}&F_{mn}(t)\\ &= \frac{e^{iwt}U[1-(-1)^m][1-(-1)^n]\nu\lambda_{mn}(1+iw\theta)}{\zeta_m\lambda_n}\sum_{p=0}^{\infty}\sum_{q=0}^{\infty}\sum_{r=0}^{\infty}\sum_{s=0}^{\infty}\sum_{l=0}^{\infty}\\ &\times\frac{\nu^{p+1}\lambda^s\theta^q K^{p-r}H^l(\lambda_{mn})^{r+1}\Gamma(q-p)\Gamma(r-p)\Gamma(s+p+1)\Gamma(l+p+1)t^{l-q+p}}{(-1)^{-(p+q+r+s+l)}q!r!s!l!\Gamma(p)\Gamma(p)\Gamma(1+p)\Gamma(1+p)\Gamma l-q+p+1}.\end{aligned} \tag{21}$$

Taking the inverse Fourier sine transform we get the analytic solution of the velocity field

$$\begin{aligned}F(x,y,t) &= \frac{4}{dh}\sum_{m=1}^{\infty}\sum_{n=1}^{\infty} sin\,(\zeta_m x)\,sin\,(\lambda_n y)F_{mn}(x,y,t)\\ &= \frac{4e^{iwt}U(1+iw\theta)}{dh}\sum_{m=1}^{\infty}\sum_{n=1}^{\infty}\frac{[1-(-1)^m][1-(-1)^n]\,sin\,(\zeta x)\,sin\,(\lambda_n y)}{\zeta_m\lambda_n}\\ &\times\sum_{p=0}^{\infty}\sum_{q=0}^{\infty}\sum_{r=0}^{\infty}\sum_{s=0}^{\infty}\sum_{l=0}^{\infty}\frac{\nu^{p+1}\lambda^s\theta^q K^{p-r}H^l(\lambda_{mn})^{r+1}t^{l-q+p}}{(-1)^{-(p+q+r+s+l)}q!r!s!l!}\\ &\times\frac{\Gamma(q-p)\Gamma(r-p)\Gamma(s+p+1)\Gamma(l+p+1)}{\Gamma(p)\Gamma(p)\Gamma(1+p)\Gamma(1+p)\Gamma l-q+p+1}.\end{aligned} \tag{22}$$

To obtain a more compact form of velocity field we write Eq. (22) in terms of Fox H-function,

$$F(x,y,t) = \frac{4e^{iwt}U(1+iw\theta)}{dh}\sum_{m=1}^{\infty}\sum_{n=1}^{\infty}\frac{sin\,(\zeta_m x)\,sin\,(\lambda_n y)[1-(-1)^m][1-(-1)^n]}{\zeta_m\lambda_n}$$
$$\times\sum_{p=0}^{\infty}\sum_{q=0}^{\infty}\sum_{r=0}^{\infty}\sum_{s=0}^{\infty}\frac{(-1)^{p+q+r+s}\nu^{p+1}\lambda^s\theta^q K^{p-r}(\lambda_{mn})^{r+1}t^{-q+p}}{q!r!s!} \tag{23}$$
$$\times H_{4,6}^{1,4}\left[Ht\,\middle|\,\begin{matrix}(1-q+p,0),(1-r+p,0),(-s-p,0),(-p,1)\\(0,1),(1-p,0),(1-p,0),(-p,0),(-p,0),(q-p,1)\end{matrix}\right].$$

or

$$F(x,y,t) = \frac{16e^{iwt}U(1+iw\theta)}{dh}\sum_{c=0}^{\infty}\sum_{e=0}^{\infty}\frac{sin\,(\zeta_c x)\,sin\,(\lambda_e y)}{\zeta_c\lambda_e}$$
$$\times\sum_{p=0}^{\infty}\sum_{q=0}^{\infty}\sum_{r=0}^{\infty}\sum_{s=0}^{\infty}\frac{(-1)^{p+q+r+s}\nu^{p+1}\lambda^s\theta^q K^{p-r}(\lambda_{ce})^{r+1}t^{-q+p}}{q!r!s!} \tag{24}$$
$$\times H_{4,6}^{1,4}\left[Ht\,\middle|\,\begin{matrix}(1-q+p,0),(1-r+p,0),(1-s-p,0),(-p,1)\\(0,1),(1-p,0),(1-p,0),(-p,0),(-p,0),(q-p,1)\end{matrix}\right],$$

where

$$\zeta_c = (2m+1)\frac{\pi}{d},\ \lambda_e = (2n+1)\frac{\pi}{h},\ c = 2m+1,\ e = 2n+1.$$

From Eq. (24), we obtain the velocity field due to cosine oscillations of the duct

$$u(x,y,t) = \frac{16U(\,cos\,(wt) - w\theta\,sin\,(wt))}{dh}\sum_{c=0}^{\infty}\sum_{e=0}^{\infty}\frac{sin\,(\zeta_c x)\,sin\,(\lambda_e y)}{\zeta_c\lambda_e}$$
$$\times\sum_{p=0}^{\infty}\sum_{q=0}^{\infty}\sum_{r=0}^{\infty}\sum_{s=0}^{\infty}\frac{(-1)^{p+q+r+s}\nu^{p+1}\lambda^s\theta^q K^{p-r}(\lambda_{ce})^{r+1}t^{-q+p}}{q!r!s!} \tag{25}$$
$$\times H_{4,6}^{1,4}\left[Ht\,\middle|\,\begin{matrix}(1-q+p,0),(1-r+p,0),(1-s-p,0),(-p,1)\\(0,1),(1-p,0),(1-p,0),(-p,0),(-p,0),(q-p,1)\end{matrix}\right],$$

and the velocity field due to sine oscillations of the duct

$$v(x,y,t) = \frac{16U(\,sin\,(wt) - w\theta\,cos\,(wt))}{dh}\sum_{c=0}^{\infty}\sum_{e=0}^{\infty}\frac{sin\,(\zeta_c x)\,sin\,(\lambda_e y)}{\zeta_c\lambda_e}$$
$$\times\sum_{p=0}^{\infty}\sum_{q=0}^{\infty}\sum_{r=0}^{\infty}\sum_{s=0}^{\infty}\frac{(-1)^{p+q+r+s}\nu^{p+1}\lambda^s\theta^q K^{p-r}(\lambda_{ce})^{r+1}t^{-q+p}}{q!r!s!} \tag{26}$$
$$\times H_{4,6}^{1,4}\left[Ht\,\middle|\,\begin{matrix}(1-q+p,0),(1-r+p,0),(1-s-p,0),(-p,1)\\(0,1),(1-p,0),(1-p,0),(-p,0),(-p,0),(q-p,1)\end{matrix}\right].$$

We use the following property of the Fox H-function [21] in the above equation

http://dx.doi.org/10.5772/intechopen.70891

$$H_{p,q+1}^{1,p}\left[-\chi\left|\begin{matrix}(1-a_1,A_1),(1-a_2,A_2),\ldots,\left(1-a_p,A_p\right)\\(1,0),(1-b_1,B_1),\ldots,\left(1-b_q,B_q\right)\end{matrix}\right.\right]$$
$$=\sum_{k=0}^{\infty}\frac{\Gamma(a_1+A_1k)\ldots\Gamma\left(a_p+A_pk\right)}{k!\Gamma(b_1+B_1k)\ldots\Gamma\left(b_q+B_qk\right)}\chi^k.$$

5. Calculation of the shear stress

We denote the tangential tensions for the cosine oscillations of the duct by $\tau_{1c}(x,y,t)$, $\tau_{2c}(x,y,t)$ and for sine oscillations by $\tau_{1s}(x,y,t)$, $\tau_{2s}(x,y,t)$.

If we introduce

$$\tau_1(x,y,t)=\tau_{1c}(x,y,t)+i\tau_{1s}(x,y,t), \tag{27}$$

$$\tau_2(x,y,t)=\tau_{2c}(x,y,t)+i\tau_{2s}(x,y,t), \tag{28}$$

in Eq. (7), we get

$$\tau_1(x,y,t)=\frac{\mu}{(1+\lambda)}\left(1+\theta\frac{\partial}{\partial t}\right)\partial_xF(x,y,t), \tag{29}$$

$$\tau_2(x,y,t)=\frac{\mu}{(1+\lambda)}\left(1+\theta\frac{\partial}{\partial t}\right)\partial_yF(x,y,t). \tag{30}$$

We apply LT to Eqs. (29) and (30), to obtain

$$\overline{\tau}_1(x,y,s)=\frac{\mu(1+\theta s)}{1+\lambda}\partial_x\overline{F}(x,y,s), \tag{31}$$

$$\overline{\tau}_2(x,y,s)=\frac{\mu(1+\theta s)}{1+\lambda}\partial_y\overline{F}(x,y,s). \tag{32}$$

Taking the inverse Fourier transform of Eq. (19) to get $\overline{F}(x,y,s)$ and then by putting it into Eq. (31), we get

$$\overline{\tau}_1(x,y,s)=\frac{4\mu(1+\theta s)}{dh(1+\lambda)}\sum_{m=1}^{\infty}\sum_{n=1}^{\infty}\frac{cos\,(\zeta_mx)\,sin\,(\lambda_ny)[1-(-1)^m][1-(-1)^n]}{[(1+\lambda)(s+H)+\nu(1+\theta s)(\lambda_{mn}+K)]}$$
$$\times\frac{U\nu\lambda_{mn}(1+iw\theta)}{\lambda_n(s-iw)}, \tag{33}$$

or

$$\overline{\tau}_1(x,y,s)=\frac{16\mu(1+\theta s)}{dh(1+\lambda)}\sum_{c=0}^{\infty}\sum_{e=0}^{\infty}\frac{cos\,(\zeta_cx)\,sin\,(\lambda_ey)U\nu\lambda_{ce}(1+iw\theta)}{\lambda_e(s-iw)[(1+\lambda)(s+H)+\nu(1+\theta s)(\lambda_{ce}+K)]}, \tag{34}$$

where

$$\zeta_c = (2m+1)\frac{\pi}{d}, \lambda_e = (2n+1)\frac{\pi}{h}, c = 2m+1, e = 2n+1.$$

We express Eq. (34) in series form in order to obtain a more suitable form of τ_1,

$$\begin{aligned}\overline{\tau}_1(x,y,s) &= \frac{16\mu U(1+iw\theta)}{dh(s-iw)}\sum_{c=0}^{\infty}\sum_{e=0}^{\infty}\frac{cos\,(\zeta_c x)\,sin\,(\lambda_e y)}{\lambda_e}\sum_{p=0}^{\infty}\sum_{q=0}^{\infty}\sum_{r=0}^{\infty}\sum_{s=0}^{\infty}\sum_{l=0}^{\infty}\\ &\times\frac{\nu^{p+1}\lambda^s\theta^q K^{p-r}H^l(\lambda_{ce})^{r+1}\Gamma(q-p-1)\Gamma(r-p)\Gamma(s+p+2)\Gamma(l+p+1)}{(-1)^{-(p+q+r+s+l)}q!r!s!l!\Gamma(p)\Gamma(p+1)\Gamma(2+p)\Gamma(1+p)s^{l-q+p+1}}.\end{aligned} \tag{35}$$

Using the inverse LT of the last equation, we obtain

$$\begin{aligned}\tau_1(x,y,t) &= \frac{16\mu e^{iwt}U(1+iw\theta)}{dh}\sum_{c=0}^{\infty}\sum_{e=0}^{\infty}\frac{cos\,(\zeta_c x)\,sin\,(\lambda_e y)}{\lambda_e}\sum_{p=0}^{\infty}\sum_{q=0}^{\infty}\sum_{r=0}^{\infty}\sum_{s=0}^{\infty}\\ &\times\sum_{l=0}^{\infty}\frac{\nu^{p+1}\lambda^s\theta^q K^{p-r}H^l(\lambda_{ce})^{r+1}t^{l-q+p}\Gamma(q-p-1)\Gamma(s+p+2)}{(-1)^{-(p+q+r+s+l)}q!r!s!l!\Gamma(p)\Gamma(p+1)\Gamma(2+p)\Gamma(1+p)}\\ &\times\frac{\Gamma(l+p+1)}{\Gamma(l-q+p+1)}.\end{aligned} \tag{36}$$

Lastly, we write the stress field in a more compact form by using Fox H-function

$$\begin{aligned}\tau_1(x,y,t) &= \frac{16\mu e^{iwt}U(1+iw\theta)}{dh}\sum_{c=0}^{\infty}\sum_{e=0}^{\infty}\frac{cos\,(\zeta_c x)\,sin\,(\lambda_e y)}{\lambda_e}\sum_{p=0}^{\infty}\\ &\times\sum_{q=0}^{\infty}\sum_{r=0}^{\infty}\sum_{s=0}^{\infty}\frac{\nu^{p+1}\lambda^s\theta^q K^{p-r}(\lambda_{mn})^{r+1}t^{-q+p}}{(-1)^{-(p+q+r+s)}q!r!s!}\\ &\times H_{4,6}^{1,4}\left[Ht\left|\begin{matrix}(2-q+p,0),(1-r+p,0),(-1-s-p,0),(-p,1)\\(0,1),(-p,0),(-1-p,0),(-p,0),(-p,0),(q-p,1)\end{matrix}\right.\right].\end{aligned} \tag{37}$$

From Eq. (37), we obtain the tangential tension due to cosine oscillations of the duct

$$\begin{aligned}\tau_{1c}(x,y,t) &= \frac{16U\mu(\,cos\,(wt)-w\theta\,sin\,(wt))}{dh}\sum_{c=0}^{\infty}\sum_{e=0}^{\infty}\frac{cos\,(\zeta_c x)\,sin\,(\lambda_e y)}{\lambda_e}\\ &\times\sum_{p=0}^{\infty}\sum_{q=0}^{\infty}\sum_{r=0}^{\infty}\sum_{s=0}^{\infty}\frac{(-1)^{p+q+r+s}\nu^{p+1}\lambda^s\theta^q K^{p-r}(\lambda_{mn})^{r+1}t^{-q+p}}{q!r!s!}\\ &\times H_{4,6}^{1,4}\left[Ht\left|\begin{matrix}(2-q+p,0),(1-r+p,0),(-1-s-p,0),(-p,1)\\(0,1),(-p,0),(-1-p,0),(-p,0),(-p,0),(q-p,1)\end{matrix}\right.\right],\end{aligned} \tag{38}$$

and the tangential tension corresponding to sine oscillations of the duct

$$\begin{aligned}\tau_{1s}(x,y,t) &= \frac{16U\mu(\,sin\,(wt)-w\theta\,cos\,(wt))}{dh}\sum_{c=0}^{\infty}\sum_{e=0}^{\infty}\frac{cos\,(\zeta_c x)\,sin\,(\lambda_e y)}{\lambda_e}\sum_{p=0}^{\infty}\\ &\times\sum_{q=0}^{\infty}\sum_{r=0}^{\infty}\sum_{s=0}^{\infty}\frac{(-1)^{p+q+r+s}\nu^{p+1}\lambda^s\theta^q K^{p-r}(\lambda_{mn})^{r+1}t^{-q+p}}{q!r!s!}\\ &\times H_{4,6}^{1,4}\left[Ht\middle|\begin{matrix}(2-q+p,0),(1-r+p,0),(-1-s-p,0),(-p,1)\\(0,1),(-p,0),(-1-p,0),(-p,0),(-p,0),(q-p,1)\end{matrix}\right].\end{aligned}\tag{39}$$

In the similar fashion we can find $\tau_{2c}(x,y,t)$ and $\tau_{2s}(x,y,t)$ from Eqs. (19) and (32).

6. Volume flux

The volume flux due to cosine oscillations is given by

$$Q_c(x,y,t)=\int_0^d\int_0^h u(x,y,t)dxdy,\tag{40}$$

putting $u(x,y,t)$ from Eq. (25) into the above equation, we obtain the volume flux of the rectangular duct due to cosine oscillations

$$\begin{aligned}u(x,y,t) &= \frac{64U(\,cos\,(wt)-w\theta\,sin\,(wt))}{dh}\sum_{c=0}^{\infty}\sum_{e=0}^{\infty}\frac{1}{(\zeta_c\lambda_e)^2}\\ &\times\sum_{p=0}^{\infty}\sum_{q=0}^{\infty}\sum_{r=0}^{\infty}\sum_{s=0}^{\infty}\frac{\nu^{p+1}\lambda^s\theta^q K^{p-r}(\lambda_{ce})^{r+1}t^{-q+p}}{(-1)^{-(p+q+r+s)}q!r!s!}\\ &\times H_{4,6}^{1,4}\left[Ht\middle|\begin{matrix}(1-q+p,0),(1-r+p,0),(1-s-p,0),(-p,1)\\(0,1),(1-p,0),(1-p,0),(-p,0),(-p,0),(q-p,1)\end{matrix}\right].\end{aligned}\tag{41}$$

Similarly, we obtain the volume flux of the rectangular duct due to the sine oscillations

$$\begin{aligned}v(x,y,t) &= \frac{64U(\,sin\,(wt)-w\theta\,cos\,(wt))}{dh}\sum_{c=0}^{\infty}\sum_{e=0}^{\infty}\frac{1}{(\zeta_c\lambda_e)^2}\\ &\times\sum_{p=0}^{\infty}\sum_{q=0}^{\infty}\sum_{r=0}^{\infty}\sum_{s=0}^{\infty}\frac{\nu^{p+1}\lambda^s\theta^q K^{p-r}(\lambda_{ce})^{r+1}t^{-q+p}}{(-1)^{-(p+q+r+s)}q!r!s!}\\ &\times H_{4,6}^{1,4}\left[Ht\middle|\begin{matrix}(1-q+p,0),(1-r+p,0),(1-s-p,0),(-p,1)\\(0,1),(1-p,0),(1-p,0),(-p,0),(-p,0),(q-p,1)\end{matrix}\right].\end{aligned}\tag{42}$$

7. Numerical results and discussion

We have presented flow problem of MHD Jeffrey fluid passing through a porous rectangular duct. Exact analytical solutions are established for such flow problem using DFFST and LT

technique. The obtained solutions are expressed in series form using Fox H-functions. Several graphs are presented here for the analysis of some important physical aspects of the obtained solutions. The numerical results show the profiles of velocity and the adequate shear stress for the flow. We analyze these results by variating different parameters of interest.

The effects of relaxation time λ of the model are important for us to be discuss. In **Figure 1** we depict the profiles of velocity and shear stress for three different values of λ. It is observed from these figures that the flow velocity as well as the shear stress decreases with increasing λ, which corresponds to the shear thickening phenomenon. **Figure 2** are sketched to show the velocity and the shear stress profiles at different values of retardation time θ. It is noticeable that velocity as well as the shear stress decreases by increasing θ. In order to study the effect of frequency of oscillation ω, we have plotted **Figure 3**, where it appears that the velocity is also a strong function of ω of the Jeffrey fluid. The effect of frequency of oscillation on the velocity profile for cosine oscillation is same as that of the retardation time θ. The effect of magnetic parameter H of the model is important for us to be discussed. In **Figure 4**,

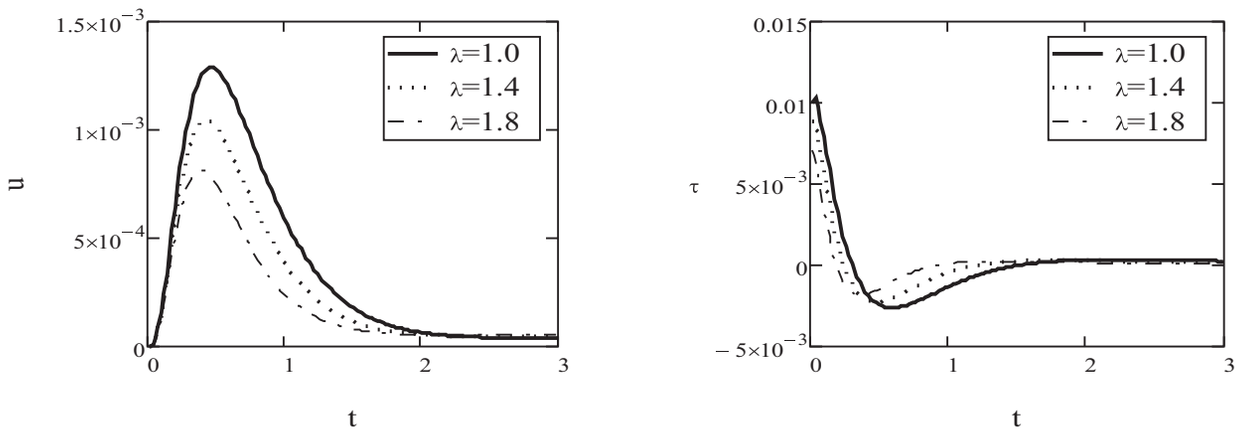

Figure 1. Velocity and shear stress profiles corresponding to the cosine oscillations of the duct for different values of λ. Other parameters are taken as $x = 0.5$, $y = 0.3$, $U = 0.2$, $H = 0.5$, $K = 0.6$, $d = 1$, $h = 2$, $\theta = 0.6$, $\omega = 0.5$ and $\nu = 0.1$.

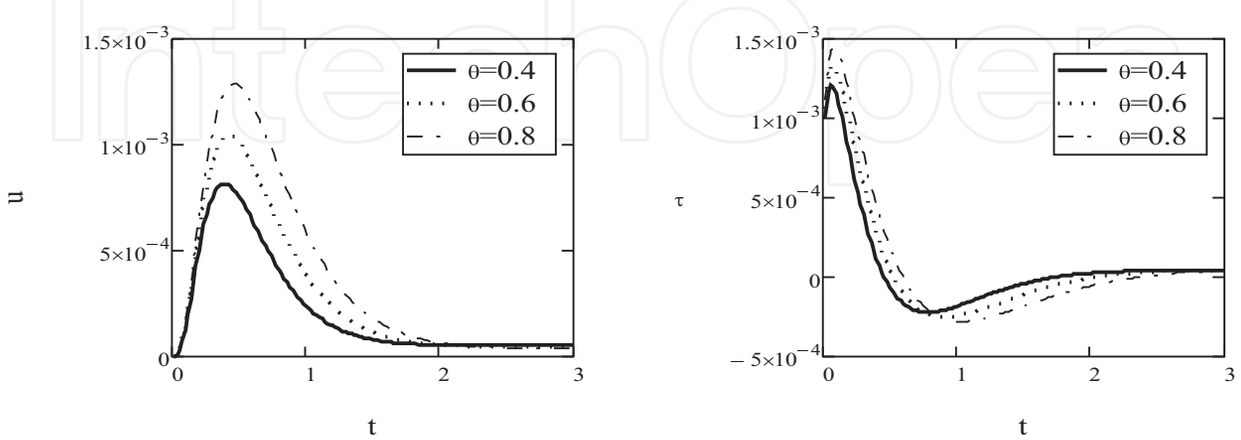

Figure 2. Velocity and shear stress profiles corresponding to the cosine oscillations of the duct for different values of θ. Other parameters are taken as $x = 0.5$, $y = 0.3$, $U = 0.2$, $H = 0.5$, $K = 0.6$, $d = 1$, $h = 2$, $\lambda = 1.4$, $\omega = 0.5$ and $\nu = 0.1$.

http://dx.doi.org/10.5772/intechopen.70891

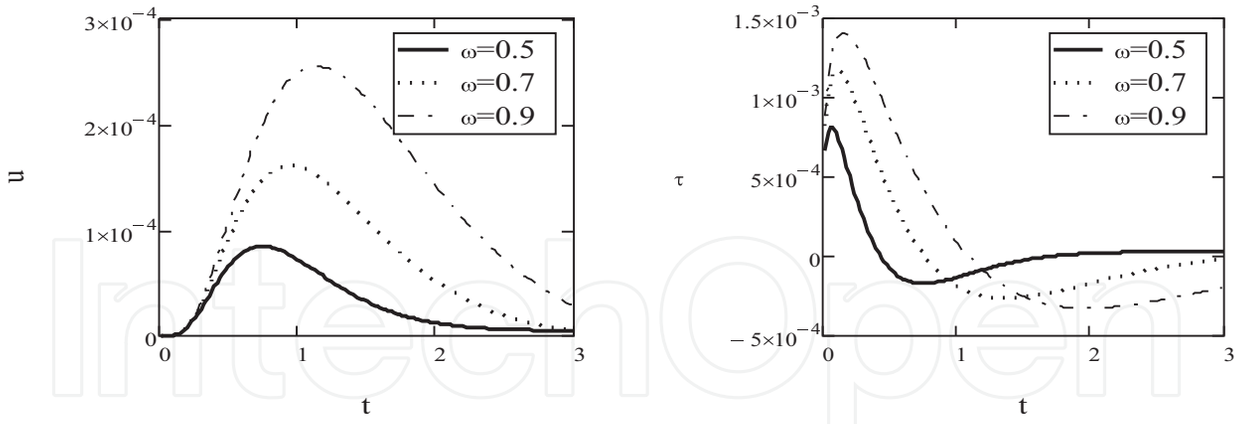

Figure 3. Velocity and shear stress profiles corresponding to the cosine oscillations of the duct for different values of ω. Other parameters are taken as $x = 0.5$, $y = 0.3$, $U = 0.2$, $H = 0.5$, $K = 0.6$, $d = 1$, $h = 2$, $\theta = 0.6$, $\lambda = 1.4$ and $\nu = 0.1$.

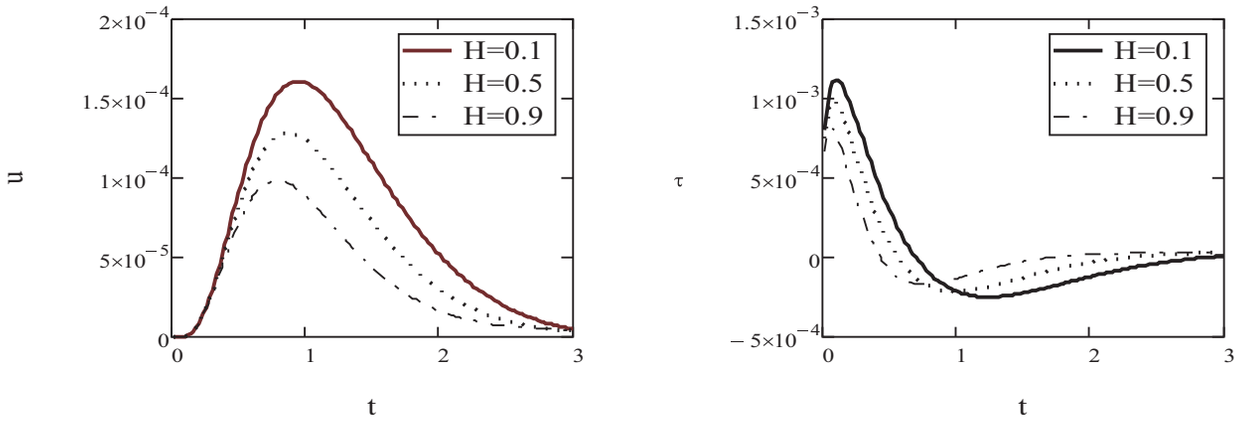

Figure 4. Velocity and shear stress profiles corresponding to the cosine oscillations of the duct for different values of H. Other parameters are taken as $x = 0.5$, $y = 0.3$, $U = 0.2$, $\lambda = 1.4$, $K = 0.6$, $d = 1$, $h = 2$, $\theta = 0.6$, $\omega = 0.5$ and $\nu = 0.1$.

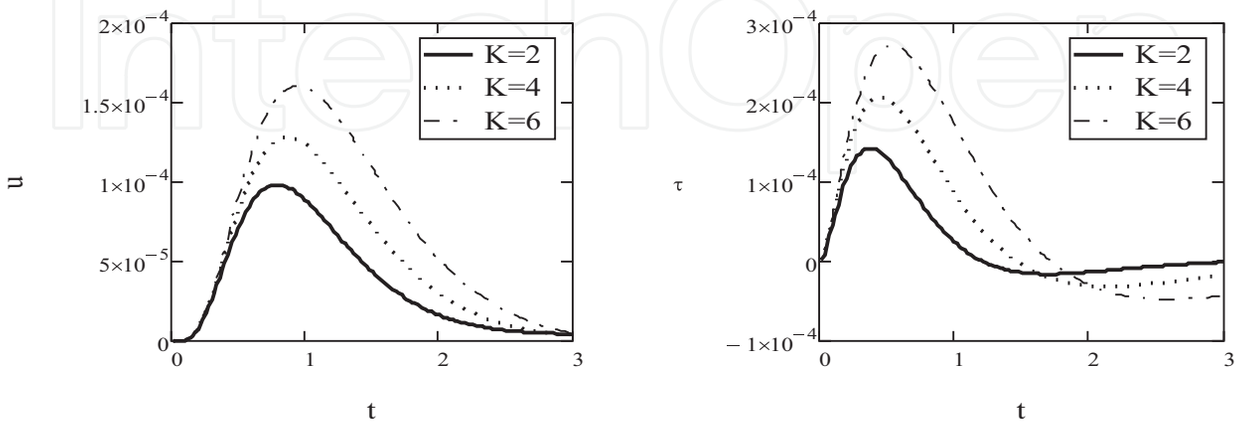

Figure 5. Velocity and shear stress profiles corresponding to the cosine oscillations of the duct for different values of K. Other parameters are taken as $x = 0.5$, $y = 0.3$, $U = 0.2$, $H = 0.5$, $\lambda = 1.4$, $d = 1$, $h = 2$, $\theta = 0.6$, $\omega = 0.5$ and $\nu = 0.1$.

we depict the profiles of velocity and shear stress for three different values of H. It is observed from these figures that the flow velocity as well as the shear stress decreases with increasing H, which corresponds to the shear thickening phenomenon. **Figure 5** is sketched to show the velocity and the shear stress profiles at different values of K. It is noticeable that velocity as well as the shear stress increases by increasing K. In order to study the effects of t, we have plotted **Figure 6**, where it appears that the velocity is also a strong function of t of the Jeffrey fluid. It can be observed that the increase of t acts as an increase of the magnitude of velocity components near the plate, and this corresponds to the shear-thinning behavior of the examined non-Newtonian fluid. **Figure 7** presents the velocity field and the shear stress profiles at different values of y. It is noticeable that velocity and shear stress both decreases by increasing y.

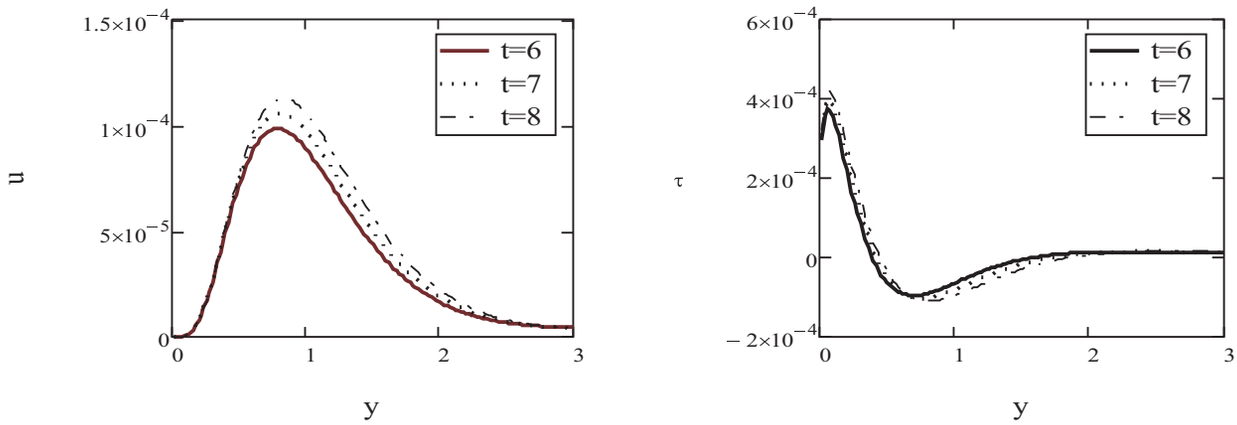

Figure 6. Velocity and shear stress profiles corresponding to the cosine oscillations of the duct for different values of t. Other parameters are taken as $x = 0.5$, $\lambda = 1.4$, $U = 0.2$, $H = 0.5$, $K = 0.6$, $d = 1$, $h = 2$, $\theta = 0.6$, $\omega = 0.5$ and $\nu = 0.1$.

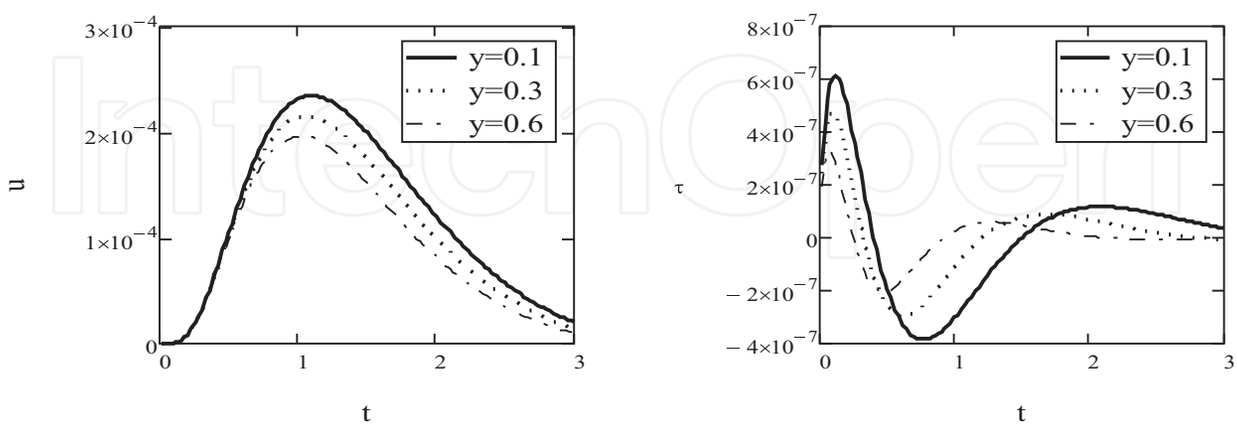

Figure 7. Velocity and shear stress profiles corresponding to the cosine oscillations of the duct for different values of y. Other parameters are taken as $x = 0.5$, $\lambda = 1.4$, $U = 0.2$, $H = 0.5$, $K = 0.6$, $d = 1$, $h = 2$, $\theta = 0.6$, $\omega = 0.5$ and $\nu = 0.1$.

Author details

Amir Khan[1,2]*, Gul Zaman[1] and Obaid Algahtani[3]

*Address all correspondence to: amir.maths@gmail.com

1 Department of Mathematics, University of Malakand, Chakdara, Dir (Lower), Khyber Pakhtunkhwa, Pakistan

2 Department of Mathematics and Statistics, University of Swat, Khyber Pakhtunkhwa, Pakistan

3 Department of Mathematics, Science College, King Saud University, Saudi Arabia

References

[1] Rajagopal KR, Srinivasa A. Exact solutions for some simple flows of an Oldroyd-B fluid. Acta Mechanica. 1995;**113**:233-239

[2] Tan WC, Masuoka T. Stoke's first problem for second grade fluid in a porous half space. International Journal of Non-Linear Mechanics. 2005;**40**:515-522

[3] Tan WC, Masuoka T. Stoke's first problem for an Oldroyd-B fluid in a porous half space. Physics of Fluids. 2005;**17**:023101

[4] Khadrawi AF, Al-Nimr MA, Othman A. Basic viscoelastic fluid problems using the Jeffreys model. Chemical Engineering Science. 2005;**60**:7131-7136

[5] Chen CI, Chen CK, Yang YT. Unsteady unidirectional flow of an Oldroyd-B fluid in a circular duct with different given volume flow rate. International Journal of Heat and Mass Transfer. 2004;**40**:203-209

[6] Nadeem S, Hussain A, Khan M. Stagnation flow of a Jeffrey fluid over a shrinking sheet. Zeitschrift für Naturforschung. 2010;**65a**:540-548

[7] Khan M. Partial slip effects on the oscillatory flows of a fractional Jeffrey fluid in a porous medium. Journal of Porous Media. 2007;**10**:473-487

[8] Hayat T, Khan M, Fakhar K, Amin N. Oscillatory rotating flows of a fractional Jeffrey fluid filling a porous medium. Journal of Porous Media. 2010;**13**(1):29-38

[9] Khan M, Iftikhar F, Anjum A. Some unsteady flows of a Jeffrey fluid between two side walls over a plane wall. Zeitschrift für Naturforschung. 2011;**66**(a):745-752

[10] Gardner LRT, Gardner GA. A two-dimensional bi-cubic B-spline finite element used in a study of MHD duct flow. Computer Methods in Applied Mechanics and Engineering. 1995;**124**:365-375

[11] Fetecau C, Fetecau C. Unsteady flows of Oldroyd-B fluids in a channel of rectangular cross-section. International Journal of Non-Linear Mechanics. 2005;**40**:1214-1219

[12] Nazar M, Shahid F, Akram S, Sultan Q. Flow on oscillating rectangular duct for Maxwell fluid. Applied Mathematics and Mechanics (English Edition). 2012;**33**:717-730

[13] Sultan Q, Nazar M, Akhtar W, Ali U. Unsteady flow of a Maxwell fluid in a porous rectangular duct. Scientific International Journal. 2013;**25**(2):181-194

[14] Tsangaris S, Vlachakis NW. Exact solution of the Navier-Stokes equations for the oscillating flow in a duct of a cross-section of right-angled isosceles triangle. Zeitschrift für Angewandte Mathematik und Physik. 2003;**54**:1094-1100

[15] Vajravelu K. Hydromagnetic flow and heat transfer over a continuous moving porous flat surface. Acta Mechanica. 1986;**64**:179-185

[16] Amakiri ARC, Ogulu A. The effect of viscous dissipative heat and uniform magnetic field on the free convective flow through a porous medium with heat generation/absorption. European Journal of Scientific Research. 2006;**15**(4):436-445

[17] Singh KD. Exact solution of an oscillatory MHD flow in a channel filled with porous medium. International Journal of Applied Mechanics and Engineering. 2011;**16**:277-283

[18] Samiulhaq, Fetecau, Khan I, Ali F, Shafie S. Radiation and porosity effects on the magnetohydrodynamic flow past an oscillating vertical plate with uniform heat flux. Zeitschrift für Naturforschung. 2012;**67**(a):572-580

[19] Khan I, Fakhar K, Shafie S. Magnetohydrodynamic free convection flow past an oscillating plate embedded in a porous medium. Journal of the Physical Society of Japan. 2011;**80**:104-110

[20] Sneddon IN. Fourier Transforms. New York: McGraw-Hill; 1951

[21] Mathai AM, Saxena RK, Haubold HJ. The H-functions: Theory and Applications. New York: Springer; 2010